

Short communication

Simulation of capacity loss in carbon electrode for lithium-ion cells during storage

Ramaraja P. Ramasamy¹, Jong-Won Lee, Branko N. Popov^{*}

*Center for Electrochemical Engineering, Department of Chemical Engineering,
University of South Carolina, Columbia, SC 29208, United States*

Received 11 December 2006; received in revised form 20 December 2006; accepted 21 December 2006
Available online 16 January 2007

Abstract

A mathematical model was developed which simulates the self-discharge capacity losses in the carbon anode for a SONY 18650 lithium-ion battery. The model determines the capacity loss during storage on the basis of a continuous reduction of organic solvent and de-intercalation of lithium at the carbon/electrolyte interface. The state of charge, open circuit potential, capacity loss and film resistance on the carbon electrode were calculated as a function of storage time using different values of rate constant governing the solvent reduction reaction.

© 2007 Elsevier B.V. All rights reserved.

Keywords: Lithium-ion battery; Carbon anode; Self-discharge; Capacity loss simulation; Storage

1. Introduction

There are several processes which cause the self-discharge capacity loss of lithium-ion batteries during storage, including internal electron leakage, dissolution of active electrode materials, corrosion of current collectors and parasitic chemical/electrochemical reactions on the electrode surfaces. It has been known [1–7] that the overall self-discharge of a lithium-ion cell is mainly controlled by the parasitic reaction of electrolyte reduction or decomposition on both graphite anode and LiCoO_2 cathode.

The parasitic reactions on the carbon anode have been taken into account in the simulation model of charge–discharge cycling of lithium-ion cells by Darling and Newman [8]. Ramadass et al. [9] and recently Ning and Popov [10] have extended the lithium intercalation model to develop a capacity fade model during cycling process on the basis of the loss of active lithium-ions due to the parasitic reactions. Besides the fact that there is considerable experimental evidence in the literature with regard to the self-discharge, there was no attempt

to simulate the self-discharge capacity loss in lithium-ion cells.

All capacity loss of a lithium-ion cell during storage is not totally irreversible: namely, a fraction of the capacity lost during storage, which is called a ‘reversible capacity loss’ ($Q_{s,rev}$), can be recovered upon subsequent charging process, and the remaining fraction that cannot be recovered is an ‘irreversible capacity loss’ ($Q_{s,irr}$). The underlying mechanism for the ‘reversible capacity loss’ is briefly presented in the following section. The capacity loss ($Q_{s,tot}$) measured at the end of storage represents the sum of $Q_{s,rev}$ and $Q_{s,irr}$, and the stored cell should be charged and then discharged, in order to experimentally distinguish between $Q_{s,rev}$ and $Q_{s,irr}$, as explained in the flowchart of Fig. 1.

The objective of this work is to develop a mathematical model which is capable of predicting the total capacity loss occurring in carbon electrode for lithium-ion cells during storage. No attempt was made to distinguish between reversible and irreversible capacity losses, since most applications (e.g. ‘back up power systems’ in satellites and space shuttles) may require the stored cell to be used ‘as-is’ without re-charging process.

2. Model development

The model assumes that the self-discharge reaction in the carbon anode involves only the solvent reduction reaction on

^{*} Corresponding author. Tel.: +1 803 777 7314; fax: +1 803 777 8265.
E-mail address: popov@enr.sc.edu (B.N. Popov).

¹ Present address: Department of Mechanical and Nuclear Engineering, Pennsylvania State University, University Park, PA 16802, United States.

Nomenclature

a	specific surface area of porous electrode (m^{-1})
C_{Li}	lithium concentration in the carbon electrode (mol m^{-3})
$C_{\text{Li,max}}$	maximum lithium concentration in the carbon electrode (mol m^{-3})
C_{P}	product (precipitate) concentration on the electrode surface (mol m^{-3})
$C_{\text{P,max}}$	maximum product (precipitate) concentration on the electrode surface (mol m^{-3})
C_{S}	solvent concentration at the electrode/electrolyte interface (mol m^{-3})
$C_{\text{S,max}}$	maximum solvent concentration at the electrode/electrolyte interface (mol m^{-3})
F	faraday constant (C mol^{-1})
J_{s}	current density for solvent reduction reaction (A m^{-2})
J_{s0}	exchange current density for solvent reduction reaction (A m^{-2})
k_0	rate constant for solvent reduction (m s^{-1})
M_{P}	molecular weight of newly formed surface film (kg mol^{-1})
$Q_{\text{s,irr}}$	irreversible capacity loss (C m^{-2})
$Q_{\text{s,rev}}$	reversible capacity loss (C m^{-2})
$Q_{\text{s,tot}}$	total capacity loss (C m^{-2})
R	gas constant ($\text{J mol}^{-1} \text{K}^{-1}$)
R_{film}	total film resistance (Ωm^2)
R_{ini}	resistance of initial SEI film (Ωm^2)
R_{P}	resistance of newly formed surface film (Ωm^2)
t	time (s)
T	absolute temperature (K)
T_{s}	total parasitic reaction time (s)
U	local equilibrium potential (V)

Greek

α	transfer coefficient for solvent reduction reaction
δ_{film}	surface film thickness (m)
η_{s}	overpotential for solvent reduction reaction (V)
κ_{P}	conductivity of newly formed surface film (S m^{-1})
ρ_{P}	density of newly formed surface film (kg m^{-3})

Subscript or superscript

a	anodic reaction
c	cathodic reaction
n	negative electrode (anode)
s	solvent reduction reaction

the electrode surface and the resulting loss of active (cyclable) lithium-ions. There are no other means of the self-discharge such as internal electron leakage, active material dissolution or corrosion of the current collectors.

From the experimental studies on the self-discharge of graphite anode, Yazami and Reynier [3,11] have suggested the ‘metastable adsorbed complex model’ for the self-discharge

reaction as follows: on the carbon electrode surface, the solid phase is in contact with the liquid electrolyte present inside the porous solid-electrolyte interphase (SEI), as illustrated in Fig. 2. During storage of a lithium-ion cell, the electrolyte percolates through the cracks of the SEI film, and lithium-ions tend to de-intercalate slowly from the carbon electrode:



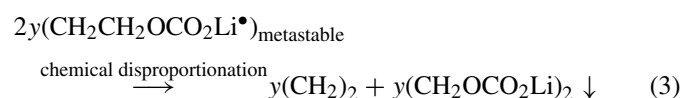
where $\text{Li}^{\infty}\text{C}_6$ is the fully charged carbon anode, $\text{Li}_{1-x}^{\infty}\text{C}_6$ the partially discharged carbon anode and $(\text{e}^{-} \cdot \text{Li}_{\theta}^{+})$ represents a pair of electron and lithium-ion localized in the SEI film resulting from the de-intercalation reaction. Under open circuit conditions the lithium de-intercalation is thermodynamically less feasible and is driven solely by the reactivity of lithium with the oxidizer present on the carbon surface.

The de-intercalated lithium-ions are consumed by a continuous formation of metastable electron-ion-electrolyte complex during storage. Such a metastable complex dissociates back to its components during the charging process of the cell after storage, and adsorbed lithium-ions on the graphite edge planes are re-intercalated into the carbon electrode. So, this reaction is responsible for a ‘reversible capacity loss’ ($Q_{\text{s,rev}}$) during storage which is recovered upon the charging process. On the other hand, a part of metastable complexes would undergo the chemical reaction which results in the formation of insoluble salts and hence the ‘irreversible capacity loss’ ($Q_{\text{s,irr}}$).

As an example, it was assumed in this study that the ethylene carbonate (EC) is reduced on the carbon anode surface to metastable complexes via two-electron transfer during storage [12]:



Then a part of metastable complexes are transformed into insoluble salts through chemical disproportionation reaction on the carbon surface during storage:



The remaining part $(1-y)$ of metastable complexes dissociate back to the original components upon the following charging step of the cell after storage. In this work, the model calculates the total capacity loss ($Q_{\text{s,tot}}$) measured during storage which is determined by reaction (2). The solvent reduction reaction is feasible at all temperatures when the anode potential is more cathodic than the reversible potential for the EC reduction reaction (0.4 V versus Li/Li⁺) [12]. It should be noted that at open circuit potential, no current flows through the external circuit and the oxidation/reduction reactions occur simultaneously within the SEI film.

The following assumptions were made for formulation of the model: (i) the solvent reduction reaction is continuous and does

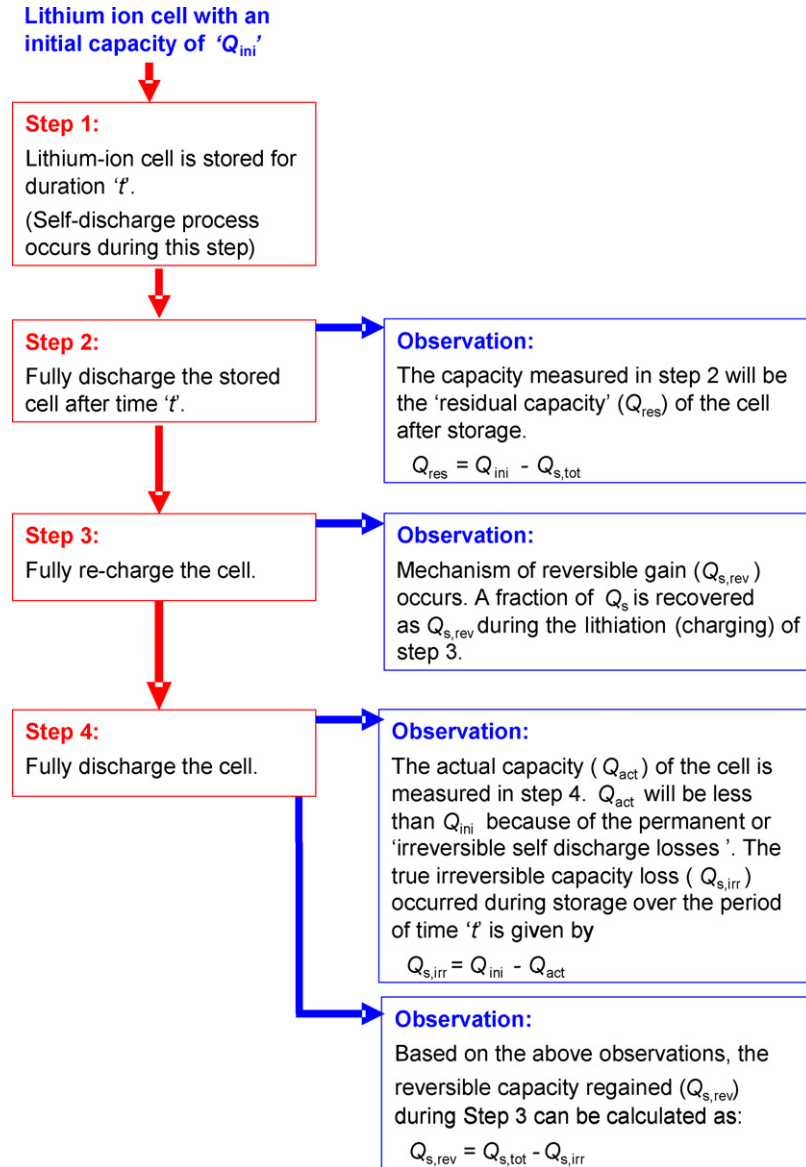


Fig. 1. Flowchart explaining the stepwise procedure for the determination of total, reversible and irreversible capacity losses during storage.

not depend on the stage transitions in the graphite electrode; (ii) the solvent reduction occurs evenly over the entire electrode surface; (iii) the solvent is present in excess at the anode/SEI film interface and thus does not limit the reduction reaction rate; (iv) there is no kinetic limitation for solvent diffusion through the cracks of the SEI film; (v) the overall self-discharge rate is so slow that it is not limited by lithium diffusion in the carbon electrode.

The rate of the solvent reduction reaction J_s on the carbon electrode surface can be expressed as

$$J_s = J_{s0} \left\{ \frac{C_s C_{Li}^2}{C_{S,max} C_{Li,max}^2} \exp\left(-\frac{\alpha_c F}{RT} \eta_s\right) - \frac{C_p}{C_{P,max}} \exp\left(\frac{\alpha_a F}{RT} \eta_s\right) \right\} \quad (4)$$

According to the assumption (v), lithium is uniformly distributed throughout the carbon particle; namely, the surface concentration of lithium is equal to the bulk concentration inside the carbon electrode. In Eq. (4), the exchange current density for solvent reduction J_{s0} depends on the initial lithium concentration in the carbon electrode:

$$J_{s0} = n F k_0 C_{Li}^{2(1-\alpha_c)} \quad (5)$$

Here, the rate constant for solvent reduction k_0 is dependent on the electrolyte composition and electrode structures in the specific battery as well as the storage temperature. The overpotential for solvent reduction η_s under open circuit conditions is expressed as:

$$\eta_s = U_n^{OCP} - U_s^{OCP} \quad (6)$$

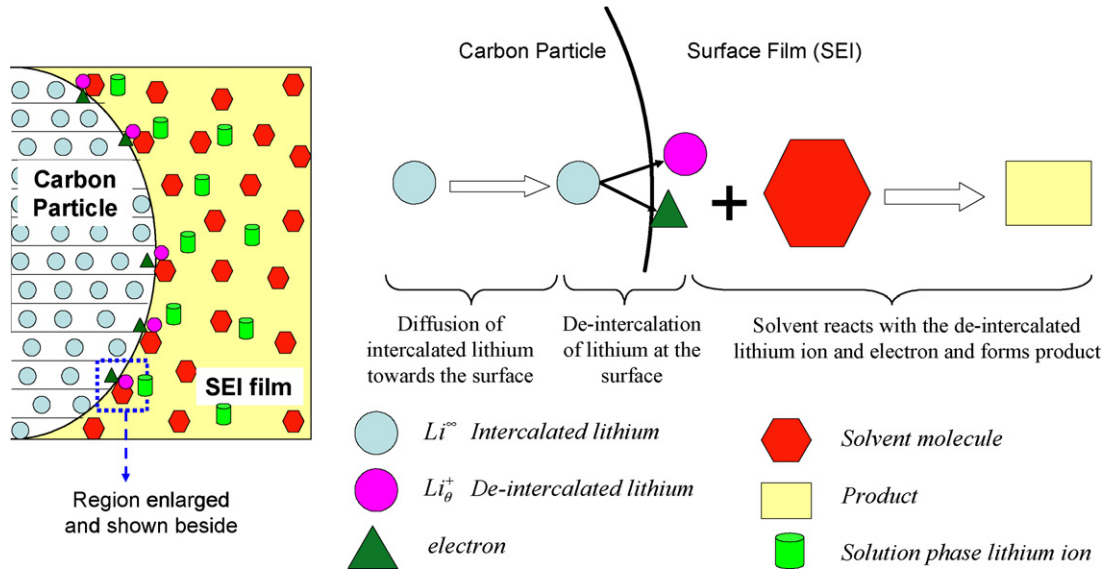


Fig. 2. Schematic diagram of the self-discharge mechanism on the carbon electrode in a lithium-ion cell.

The discharge curve of the carbon electrode taken from a SONY 18650 lithium-ion cell was measured at a C/50 rate in a three-electrode electrochemical cell with the lithium reference and counter electrodes, and then the functional expression of U_n^{OCP} was obtained by a non-linear fitting of the experimental discharge curve, as given in the Appendix.

Since the potential window of interest is far from the reversible potential for EC reduction, it is reasonable to model the solvent reduction reaction with Tafel kinetics [8,9] as follows:

$$J_s = J_{s0} \left\{ \frac{C_S C_{Li}^2}{C_{S,max} C_{Li,max}^2} \exp \left(-\frac{\alpha_c F}{RT} \eta_s \right) \right\} \quad (7)$$

Based on the assumptions (iii) and (iv), Eq. (7) reduces to

$$J_s = J_{s0} \left\{ \left(\frac{C_{Li}}{C_{Li,max}} \right)^2 \exp \left(-\frac{\alpha_c F}{RT} \eta_s \right) \right\} \quad (8)$$

Since the lithium concentration depletes as fast as the solvent reduces, the following boundary condition was used for numerical calculation:

$$-\frac{1}{a} \frac{dC_{Li}}{dt} = \frac{J_s}{nF} \quad (9)$$

The loss of active lithium-ions $Q_{s,tot}$ per unit surface area of carbon particle during storage was estimated using the following equation:

$$Q_{s,tot} = \int_0^{T_s} J_s dt \quad (10)$$

The total resistance of the SEI film, R_{film} , on the carbon electrode is the sum of the time-invariant resistance R_{ini} of the initial SEI film formed during the formation period and the time-dependent resistance R_p of the SEI film which is newly formed during

Table 1
Key parameters used in the simulation model [9]

Parameter	Unit	Value
Specific surface area of porous electrode, a	m^{-1}	3.0×10^6
Maximum lithium concentration in the carbon electrode, $C_{Li,max}$	$mol\ m^{-3}$	3.056×10^4
Molecular weight of surface film, M_p	$kg\ mol^{-1}$	7.3×10^4
Reversible potential for solvent reduction, U_s^{OCP}	V vs. Li/Li ⁺	0.4
Transfer coefficient for solvent reduction, α_c	–	0.5
Conductivity of surface film, κ_p	$S\ m^{-1}$	1
Density of surface film, ρ_p	$kg\ m^{-3}$	2.1×10^3

storage:

$$R_{film}(t) = R_{ini} + R_p(t) \quad (11)$$

where

$$R_p(t) = \frac{1}{a} \frac{\delta_{film}}{\kappa_p} \quad (12)$$

The thickness of the SEI film increases continuously over time due to the electrolyte reduction reaction:

$$\frac{\partial \delta_{film}}{\partial t} = \frac{J_s M_p}{n \rho_p F} \quad (13)$$

The key parameters used in the model are listed in Table 1.

3. Results and discussion

The model predictions were performed based on the experimental data obtained for the carbon anode taken from a SONY 18650 lithium-ion cell [13,14]. The electrochemical exper-

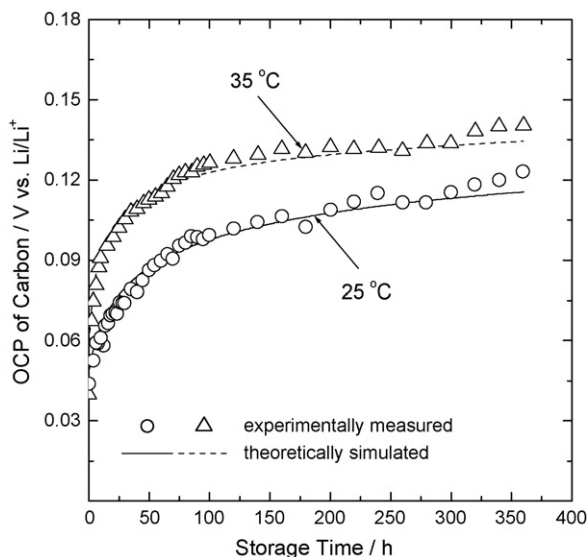


Fig. 3. Plots of OCP of the carbon electrode against storage time measured experimentally (symbol) and simulated theoretically (line). The simulations were performed with $k_0 = 1.5 \times 10^{-18}$ and $1 \times 10^{-17} \text{ m s}^{-1}$ at 25 and 35 °C, respectively.

iments were conducted in a three-electrode electrochemical cell (T-cell) with the lithium reference and counter electrodes. The electrolyte used was 1 M LiPF₆-EC/PC (50:50 vol%). Initially, the carbon electrodes were fully lithiated at 30 mV versus Li/Li⁺, followed by 1-h rest to ensure that the potential reaches its equilibrium value. Next, the OCPs were monitored as a function of storage time at different temperatures of 25 and 35 °C.

Fig. 3 shows the plots of the open circuit potential (OCP) of the carbon electrode against storage time measured experimentally and simulated theoretically. In the model, the rate of solvent reduction reaction J_s on the carbon electrode was

assumed to be given by the Tafel equation (Eq. (8)), and the value of rate constant k_0 was used as an adjustable parameter. As shown in Fig. 3, it was found that the OCP values calculated with $k_0 = 1.5 \times 10^{-18}$ and $1 \times 10^{-17} \text{ m s}^{-1}$ give the best fit to the experimental data for 25 and 35 °C, respectively. In fact, such k_0 values yield the initial exchange current densities $J_{s0}|_{t=0}$ which are in agreement with those given in literature [9]. The model does not fit the experimental data exactly at time $t=0$. The initial condition used for the model is 100% state of charge (SOC) for the carbon electrode. In practice, however, the carbon electrode cannot be fully lithiated to its theoretical maximum value, and hence the experimental data at $t=0$ show higher OCPs than those predicted by the model.

The lithium concentration in the carbon electrode was determined as a function of storage time by running the model with various values of k_0 , and the simulation results were presented in Fig. 4(a) for a period of 1 year. The carbon electrode, before undergoing the self-discharge, was completely lithiated, i.e. SOC = 100%. As shown in Fig. 4(a), the self-discharge rate of the carbon electrode is very high in the initial stage of storage and then levels off for longer storage time. The SOC decreases with storage time faster for higher k_0 value, due to higher reactivity of lithium with the solvents. Under open circuit conditions, the potential of the carbon electrode is determined solely by the solid phase concentration of lithium. Fig. 4(b) shows the OCP values of the carbon electrode simulated as a function of storage time for different k_0 values. The OCP value increases more rapidly with storage time for higher k_0 value due to higher de-intercalation rate of lithium from the carbon electrode, as described in Fig. 4(a).

Fig. 5 illustrates the OCP of the carbon electrode simulated as a function of SOC for 5 years of storage. The simulation predicts a decrease of SOC from 100 to 9% and an increase of OCP from 0.047 to 0.249 V versus Li/Li⁺ after 5 years of storage.

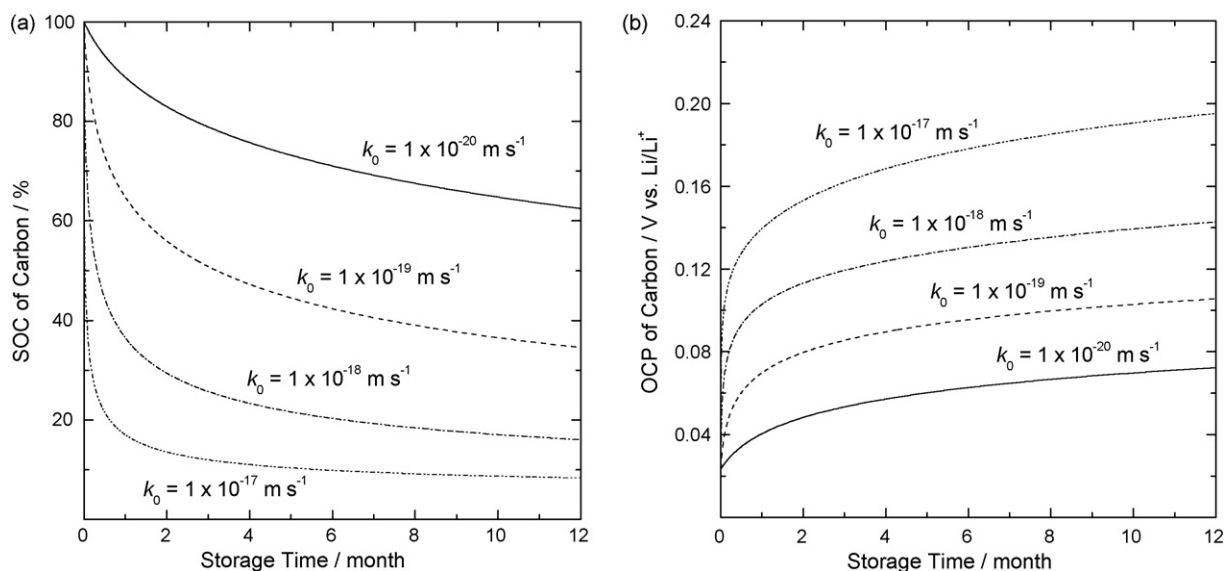


Fig. 4. Plots of (a) SOC and (b) OCP of the carbon electrode against storage time simulated with different k_0 values.

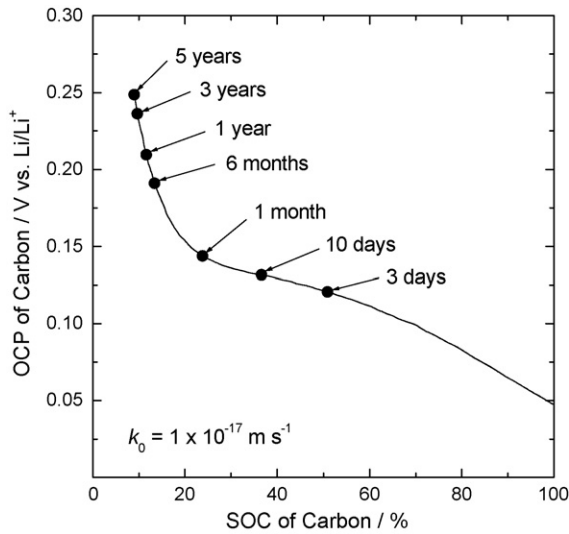


Fig. 5. OCP of the carbon electrode simulated as a function of SOC for 5 years of storage. The simulation was performed with $k_0 = 1 \times 10^{-17} \text{ m s}^{-1}$.

Fig. 6 presents the solvent reduction rate J_s calculated as a function of storage time using different k_0 values. As expected, the higher the k_0 value is, the higher is the initial J_s value; however, J_s decreases with storage time at a faster rate for higher k_0 value. For storage periods longer than 15 days, the J_s value for $k_0 = 1 \times 10^{-18} \text{ m s}^{-1}$ is lower than that for $k_0 = 1 \times 10^{-19} \text{ m s}^{-1}$. This is due to the fact that for higher k_0 the lithium concentration in the carbon/electrolyte interface depletes at a faster rate and reaches very low values within a short period of storage time, as shown in Fig. 4(a).

Fig. 7 shows the capacity loss $Q_{s,tot}$ and the film resistance R_p simulated for a period of 1 year as a function of storage time using different k_0 values. The model predicts a continuous increase in the capacity loss and film resistance with storage time. From Eqs. (10) to (13), it is

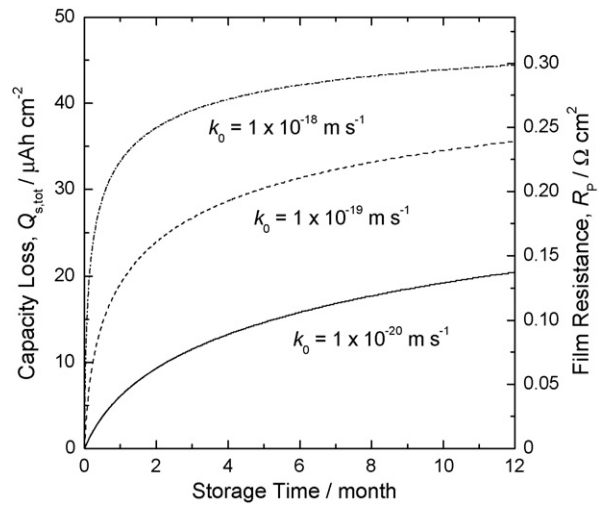


Fig. 7. Plots of capacity loss $Q_{s,tot}$ and film resistance R_p against storage time simulated for different k_0 values.

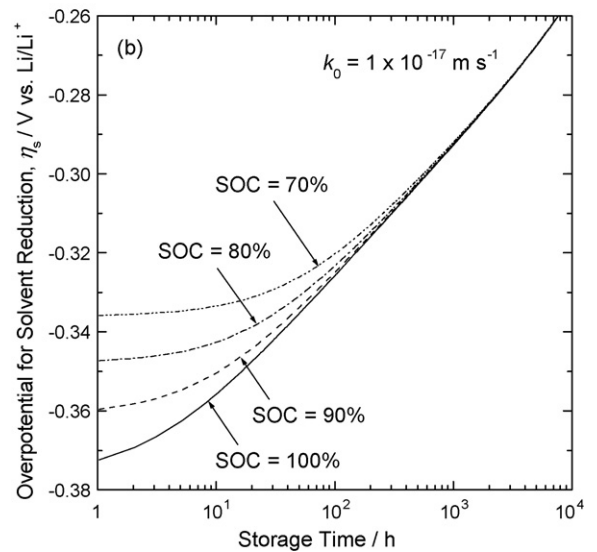
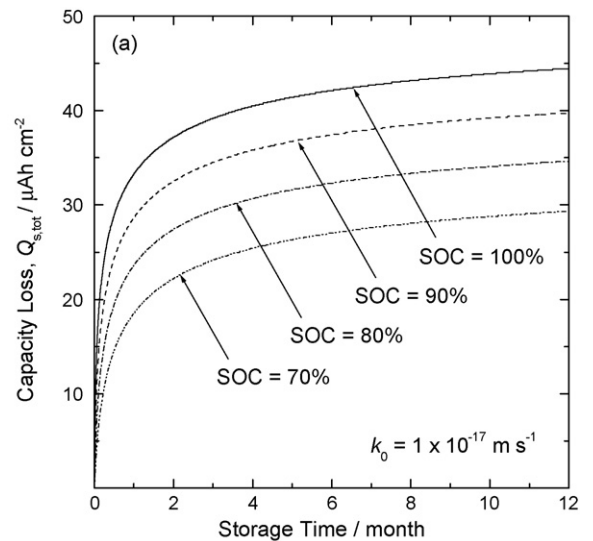


Fig. 8. Plots of (a) capacity loss due to the self-discharge of the carbon electrode and (b) overpotential for solvent reduction as a function of storage time, simulated for different initial SOC values.

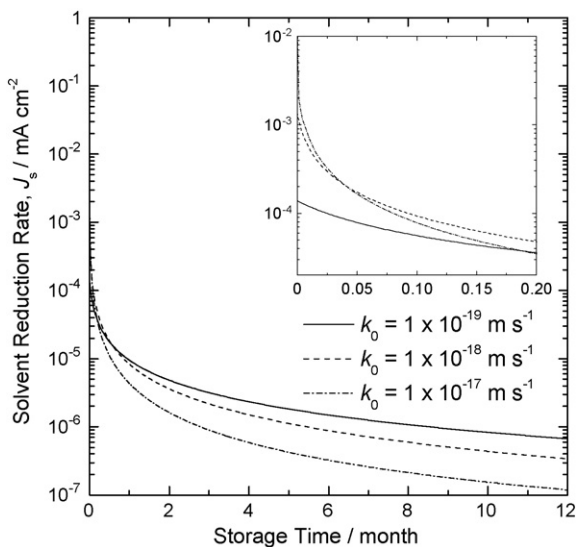


Fig. 6. Plots of solvent reduction rate J_s against storage time simulated using various k_0 values.

noted that R_p is linearly proportional to $Q_{s,tot}$ in the carbon electrode.

Fig. 8(a) presents the capacity loss $Q_{s,tot}$ due to the self-discharge of the carbon electrode simulated for different initial SOC. For the same value of $k_0 = 1 \times 10^{-17} \text{ m s}^{-1}$, the capacity loss increases with increasing the initial SOC value. The results can be explained by taking into account that the OCP of the carbon electrode U_n^{OCP} with higher SOC is more cathodic to the solvent reduction potential U_s^{OCP} than that of the electrode with lower SOC. In other words, the overpotential for the solvent parasitic reaction increases with an increase of the SOC of the carbon electrode, as presented in Fig. 8(b).

4. Conclusion

The mathematical model developed in this study predicts the capacity loss of the carbon electrode during storage due to a continuous reduction of organic solvent and de-intercalation of lithium at the carbon/electrolyte interface. The SOC, OCP, capacity loss and film resistance on the carbon electrode were simulated as a function of storage time using different values of rate constant for solvent reduction k_0 . The effect of initial SOC on the capacity loss was also studied. The simulated values of OCP were found to be in good agreement with the experimental values obtained for the carbon electrode in a SONY 18650 lithium-ion cell. In the following work, the self-discharge model presented in this study will be combined with the capacity fade cycling model [10], in order to analyze the calendar life of lithium-ion batteries during intermittent cycling process.

Appendix A

The U_n^{OCP} expression for the carbon electrode taken from a SONY 18650 cell is given by

$$\begin{aligned}
 U_n^{OCP} = & 0.7222 + 0.1387 \left(\frac{C_{Li}}{C_{Li,max}} \right) + 0.029 \left(\frac{C_{Li}}{C_{Li,max}} \right)^{0.5} \\
 & - 0.0172 \left(\frac{C_{Li}}{C_{Li,max}} \right)^{-1} + 0.0019 \left(\frac{C_{Li}}{C_{Li,max}} \right)^{-1.5} \\
 & + 0.2802 \exp \left\{ 0.9 - 15 \left(\frac{C_{Li}}{C_{Li,max}} \right) \right\} \\
 & - 0.7984 \exp \left\{ 0.4465 \left(\frac{C_{Li}}{C_{Li,max}} \right) - 0.4108 \right\} \quad (A.1)
 \end{aligned}$$

References

- [1] P. Arora, R.E. White, M. Doyle, J. Electrochem. Soc. 145 (1998) 3647.
- [2] M. Broussely, S. Herreyre, P. Biensan, P. Kaszlejna, K. Nechev, R.J. Staniewicz, J. Power Sources 97-98 (2001) 13.
- [3] R. Yazami, Y.F. Reynier, Electrochim. Acta 47 (2002) 1217.
- [4] C. Wang, X. Zhang, A.J. Appleby, X. Chen, F.E. Little, J. Power Sources 112 (2002) 98.
- [5] Y. Reynier, R. Yazami, B. Fultz, Proceedings of The 17th Annual Battery Conference on Applications and Advances, Long Beach, California, 2002, pp. 145–150.
- [6] D. Ostrovskii, F. Ronci, B. Scrosati, P. Jacobsson, J. Power Sources 94 (2001) 183.
- [7] S.H. Choi, J. Kim, Y.S. Yoon, J. Power Sources 138 (2004) 283.
- [8] R. Darling, J. Newman, J. Electrochem. Soc. 145 (1998) 990.
- [9] P. Ramadass, B. Haran, P.M. Gomadam, R.E. White, B.N. Popov, J. Electrochem. Soc. 151 (2004) A196.
- [10] G. Ning, B.N. Popov, J. Electrochem. Soc. 151 (2004) A1584.
- [11] R. Yazami, Electrochim. Acta 45 (1999) 87.
- [12] D. Aurbach, Advances in Lithium Ion Batteries, Kluwer/Plenum Publishers, 2002.
- [13] R.P. Ramasamy, P. Ramadass, B.S. Haran, B.N. Popov, J. Power Sources 124 (2003) 155.
- [14] R.P. Ramasamy, R.E. White, B.N. Popov, J. Power Sources 141 (2005) 298.